An Exact Prediction Method of Flow Stresses of Aluminum, Al-Mg-Si Alloy and SUS304 Stainless Steel

Kenji NAKANISHI, Shunpei KAMITANI, and Yasuyoshi FUKUI

(Received May 31, 1994)

ABSTRACT

Detailed analyses and forming simulations are carried out to achieve successful and optimum metal forming processes. These analyses and simulations require constitutive equations representing flow stresses at strains of a forming material in actual complex deformation conditions involving some variations of strain-rate and temperature during deformation. Nakanishi had previously proposed a numerical calculation method for predicting the flow curves by using the work-hardening rate equations. The method was applied to flow curve prediction of Aluminum, Al-Mg-Si alloy and SUS304 stainless steel, and the computer program of flow curve prediction was constructed. The program is available to predict the flow stresses of the above materials and temperature rises due to applied forming energy in the cold, warm and hot forming processes.

1. Introduction

A method of flow stress prediction should be prepared to proceed the stress analyses or numerical simulations of the metal forming processes. It is well known that the deformation conditions such as strain, strain-rate and temperature are all varying in the forming processes. Experimental results reveal that flow stresses at strains are changed in many metals and alloys with deformation condition involving strain-rate variation and temperature variation in a forming process. Much effort[1)-9)] has been done to establish a method of flow stress prediction under the above realistic deformation conditions. Nakanishi had proposed the work-hardening rate equations, so that the instantaneous effects of strain, strain-rate and temperature on flow stress can be expressed by mathematical equations. Furthermore, the numerical calculation method for predicting the flow curves by using the work-hardening rate equations had been developed[4),5)]. The method can be applied to predict the flow stresses at strains in deformation with varying strain-rate and varying temperature.

In the present investigation, the method was applied to exact prediction of flow curves of Aluminum (1100-0 aluminum), Al-Mg-Si alloy (6063 aluminum alloy) and SUS304 stainless steel, and the computer program of flow curve prediction was constructed.

2. Work-hardening rate equations and flow curve prediction

Flow curves or uniaxial compressive stress and strain curves of metals and alloys are complex functions of strain, strain-rate and temperature, and affected with deformation pass his-

tory.

The instantaneous effects of strain, strain-rate and temperature on flow stress in a deformation process can be described mathematically by the work-hardening rate equations. The equations of work-hardening rate were formulated from the rate theory of work-hardening and dynamic recovery. Some material constants involved in the work-hardening rate equations can be determined by numerical analysis referring to the flow curves measured by experiments.

$$\left(\frac{d\sigma}{d\varepsilon}\right)_{\varepsilon,\dot{\varepsilon},T} = \left(\frac{d\sigma_m}{d\varepsilon}\right)_{\varepsilon,\dot{\varepsilon},T_o} - \frac{\gamma_o}{\dot{\varepsilon}}(\sigma_m'-\sigma)\exp(q\sigma^2) \quad \cdots\cdots (1)$$

$$\left(\frac{d\sigma_m}{d\varepsilon}\right)_{\varepsilon,\dot{\varepsilon},T_o} = \left(\frac{d\sigma_o}{d\varepsilon}\right)_{\varepsilon,\dot{\varepsilon}_b,T_o} + \frac{\gamma_s}{\dot{\varepsilon}}|(\sigma_o'-\sigma_m)| \quad \cdots\cdots (2)$$

$$\sigma_m' = \sigma_{\varepsilon i} + \int_{\varepsilon i}^{\varepsilon i+\Delta\varepsilon}\left(\frac{d\sigma_m}{d\varepsilon}\right)_{\varepsilon,\dot{\varepsilon},T_o} d\varepsilon \quad \cdots\cdots (3)$$

$$\sigma_o' = \sigma_{\varepsilon i} + \int_{\varepsilon i}^{\varepsilon i+\Delta\varepsilon}\left(\frac{d\sigma_o}{d\varepsilon}\right)_{\varepsilon,\dot{\varepsilon}_b,T_o} d\varepsilon$$

$$= (\sigma_b)_{\varepsilon i+\Delta\varepsilon} - (\sigma_b)_{\varepsilon i} + \sigma_{\varepsilon i} \quad \cdots\cdots (4)$$

($\sigma_b-\varepsilon$ curve)$_{\dot{\varepsilon}_b,T_o}$

$$\left(\frac{d\sigma_o}{d\varepsilon}\right)_{\varepsilon,\dot{\varepsilon}_b,T_o} = \left(\frac{d\sigma_b}{d\varepsilon}\right)_{\varepsilon,\dot{\varepsilon}_b,T_o} \quad \cdots\cdots (5)$$

$$\Delta t_e = \frac{\beta}{Jc\rho}\int_{\varepsilon i}^{\varepsilon i+\Delta\varepsilon}\sigma d\varepsilon \quad \cdots\cdots (6)$$

Eqs. (1) and (2) are the work-hardening rate equations proposed previously. Eqs. (3)–(6) are the supplemental equations for calculating the flow curves by using eqs. (1) and (2).

Eq. (1) is the work-hardening rate equation of a metal or an alloy being deformed at elevated temperatures above base temperature, T_o. The equation explains that the work-hardening rate, $(d\sigma/d\varepsilon)_{\varepsilon,\dot{\varepsilon},T}$, measured at strain ε, strain-rate $\dot{\varepsilon}\,s^{-1}$ and temperature TK (or t_e℃) is the result of the base work-hardening rate, $(d\sigma_m/d\varepsilon)_{\varepsilon,\dot{\varepsilon},T_o}$, measured at $\varepsilon,\dot{\varepsilon}$ and base temperature T_o, minus relative dynamic recovery rate, $(\gamma_o/\dot{\varepsilon})(\sigma_m'-\sigma)\exp(q\sigma^2)$ at $\varepsilon,\dot{\varepsilon}$ and T, $(T>T_o)$. Relative dynamic recovery rate term could be formulated from the rate theory of recovery in which recovery process is considered as the thermally activated process. (The value of relative dynamic recovery rate term is 0 at base temperature, T_o.) Parameter, γ_o, is a material constant meaning $\gamma_o=k\exp(-Q_o/RT)$. Where, k means a rate sensitivity, Q_o an activation energy for self-diffusion, R a constant (8.32 J/molK) and T deformation temperature. Parameter, q, is a stress sensitivity and a material constant.

Eq. (2) is the base temperature work-hardening rate equation which is adopted to evaluate the values of the base work-hardening rate term, $(d\sigma_m/d\varepsilon)_{\varepsilon,\dot{\varepsilon},T_o}$, and reference stress, σ_m', involved in eq. (1). The term, $(d\sigma_o/d\varepsilon)_{\varepsilon,\dot{\varepsilon}_b,T_o}$, is the work-hardening rate at strain ε measured by deformation proceeded at base strain-rate, $\dot{\varepsilon}_b$, and base temperature, T_o. Where, base strain-rate, $\dot{\varepsilon}_b$, is a constant value fixed to some arbitrary value. The term, $(\gamma_s/\dot{\varepsilon})|(\sigma_o'-\sigma_m)|$, is the relative dynamic hardening rate (in which, $\gamma_s>0$) or relative dynamic recovery rate (in which, $\gamma_s<0$). Material constant, γ_s, is a strain-rate dependent and its value is 0 at base strain-rate, $\dot{\varepsilon}_b$.

In numerical calculation for predicting the flow curves, reference stresses, σ_m' in eq. (1) and σ_o' in eq. (2), should be corrected by a small strain increment, $\Delta\varepsilon$, in order to take into ac-

count the deformation path history. Stress, σ_m', is the base stress to evaluate the value of relative recovery, $(\sigma_m'-\sigma)$, and is treated as the constant value in the strain increment, $\varepsilon_i+\Delta\varepsilon$. σ_m' is calculated by eqs. (2)–(5). Base stress, σ_o' in eq. (2), in the same strain increment, $\varepsilon_i+\Delta\varepsilon$, is calculated by eq. (4). Strain increment, $\Delta\varepsilon$, in eqs. (3) and (4) coincides with strain increment in numerical integration by Runge-Kutta-Gill method. Strain increment, $\Delta\varepsilon$, in numerical calculation is set to $\Delta\varepsilon=0.004$ which is verified to achieve accurate calculation. Temperature rise due to plastic working energy is calculated by eq. (6), where, β is conversion facter, ($\beta=0$ in isothermal deformation and $\beta=1$ in adiabatic deformation), J the mechanical equivalent of heat, ($J=4.2J/cal$), c and ρ specific heat and density of a material respectively. Fig. 1 shows the flow chart of the computer prediction program of flow stresses and deformation temperatures. Input data are strain-rate variation and temperature variation in a deformation process. Numerical calculation by Runge-Kutta-Gill method in strain increment, $\Delta\varepsilon$, is performed by two steps; i.e., σ_m' in strain-range, $\varepsilon_i\sim\varepsilon_i+\Delta\varepsilon$, and the values of $(d\sigma_m/d\varepsilon)$ at strains, ε_i, $\varepsilon_i+\Delta\varepsilon/2$ and $\varepsilon_i+\Delta\varepsilon$ are calculated first by eqs. (2)–(5) and $\sigma_b-\varepsilon$ curve. Then, the values of σ and t_e at $\varepsilon_i+\Delta\varepsilon$ are calculated by eqs. (1) and (6). The equations representing the following relations listed below must be included in the program.

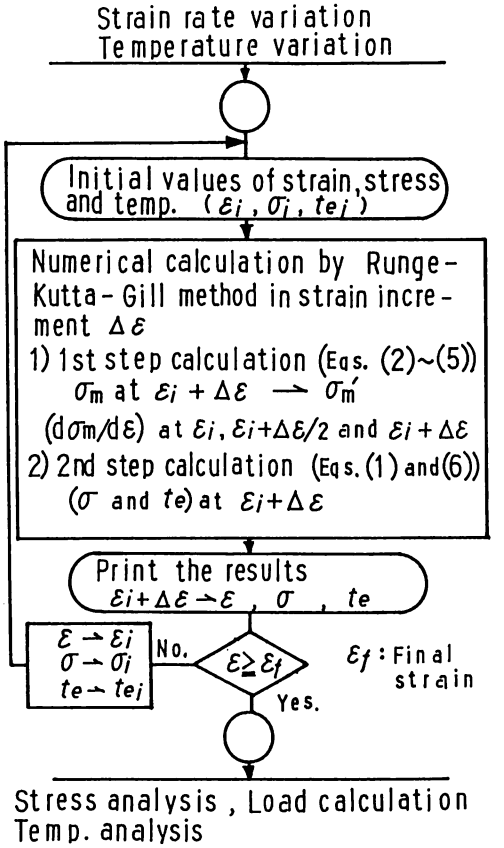

Fig. 1 Flow chart of the prediction program of flow stress and deformation temperature.

(a) σ_b–strain, ε, relation

(b) γ_s–strain-rate, $\dot{\varepsilon}$, relation

(c) γ_o–(temperature, T or t_e, and strain-rate, $\dot{\varepsilon}$), relation

(d) q–temperature, T or t_e, relation

Where, (a) is the relation measured by experiment and the relations, (b)–(d), can be determined by numerical analyses explained in chapter 3 with referring to the stress-strain curves measured by experiments.

3. Procedure to determine the material constants, γ_s, γ_o and q

Fig. 2 shows the flow chart explaining the determination procedures of the material constants, γ_s, γ_o and q. Fig. 3 represents the figures explaining the sequences of the analytic procedure for determining the values of material constants, γ_o, q and (γ_s). Determination of material constants at a deformation condition, strain-rate $\dot{\varepsilon}$ and temperature T, is explained below.

First, n data pairs, $(\sigma_i, (d\sigma/d\varepsilon)_i)$ at strain ε_i (i=1..n), are prepared from the stress-strain curve measured by experiment performed at temperature T and strain-rate $\dot{\varepsilon}$, (T and $\dot{\varepsilon}$ are con-

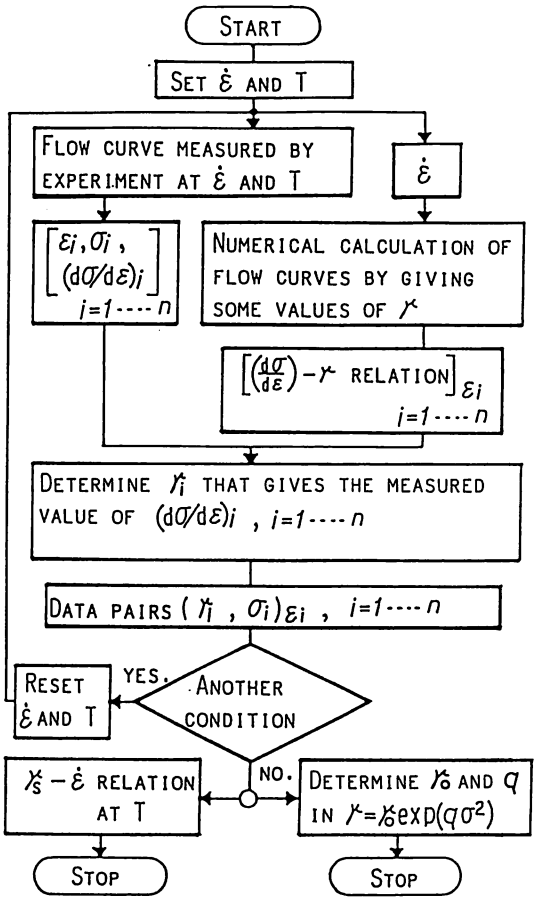

Fig. 2 Flow chart of the determination procedures of the material constants, γ_s, γ_o and q.

stant values during deformation). ((A) in Fig. 3) While, some flow curves and work-hardening rate curves, ($\sigma-\varepsilon$ curves and $(d\sigma/d\varepsilon)-\varepsilon$ curves), are calculated by using the computer prediction program shown by Fig. 1, in which $\gamma_0 \exp(q\sigma^2)$ is replaced with one unknown parameter,

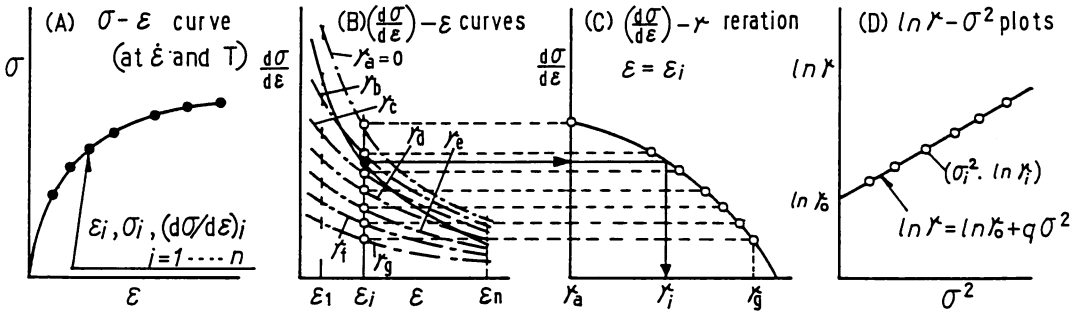

Fig. 3 Figures explaining the sequences of the analytic procedure for determining the values of material constants, γ_0, q and (γ_s).

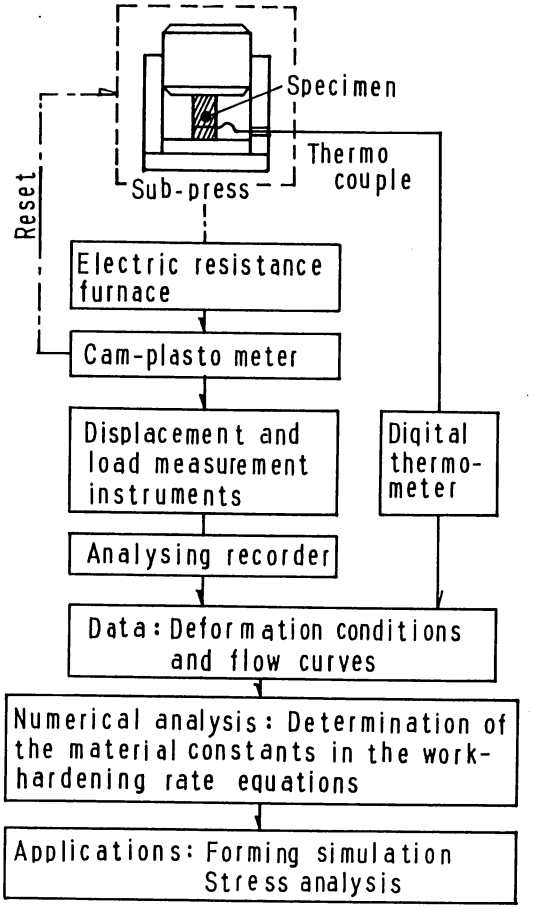

Fig. 4 Flow chart explaining the data acquisition and manipulation for determining the values of material constants involved in the work-hardening rate equations.

γ, and the calculations are proceeded by giving some values of γ, ($\gamma=\gamma_a...\gamma_g$). ((B) in Fig. 3) Then, $(d\sigma/d\varepsilon)-\gamma$ relations at some strains, ε_i, can be determined. ((C) in Fig. 3) Proper value of γ_i which produces the same value of $(d\sigma/d\varepsilon)$ as that measured by experiment can be determined from the $(d\sigma/d\varepsilon)-\gamma$ relation at strain ε_i. ((C) in Fig. 3) The above procedures are proceeded at some strains, ε_i (i=1...n), and n data pairs (γ_i, σ_i) specified at T and $\dot{\varepsilon}$ are obtained. Data pairs, (γ_i, σ_i), are plotted on $ln\gamma-\sigma^2$ relation, and linear relation, $ln\gamma=ln\gamma_o+q\sigma^2$, is obtained. Then, the values of the material constants, γ_o and q, specified at T and $\dot{\varepsilon}$ can be determined. ((D) in Fig. 3)

The above procedures are proceeded at another strain-rate and temperature combinations. Material constant, γ_s in eq. (2) can be determined by the same procedures as described above and with referring to the flow curves measured by experiments performed at some constant strain-rates at base temperature, T_o. (The value of dynamic recovery rate term in eq. (1) is 0 at base temperature, T_o.) Then, the value of γ_s can be determined with regard to strain-rates. In the above procedures, $\gamma_s-\dot{\varepsilon}$ relation should be determined first, so that 1st. step calculation in Fig. 1 is made available. Then, material constants, γ_o and q, are determined.

In the present work, semi-automated computer program of the above analysis was adopted to determine material constants. Fig. 4 shows the flow chart explaining the data acquisition and manipulation for determining the material constants involved in the work-hardening rate equations.

4. Flow curve prediction of Aluminum, Al-Mg-Si alloy and SUS304 stainless steel

4.1 Flow curves, (Uniaxial compressive stress-strain curves)

Table 1 shows chemical compositions and preparation scheme of the test pieces. Uniaxial compressive testings were performed at some temperatures above room temperature by using cam-plasto meter. Sub-press having large heat capacity was employed so that isothermal com-

Table 1 Materials and specimens

1) Aluminum (1100-0 aluminum)

Elements	Si	Mn	Ti	Fe	Zn	Cr	Cu	Mg	Al
Mass %	0.04	<0.01	<0.01	0.02	0.01	<0.01	0.01	0.01	Bal.

Cold rolled aluminum plate — Cylindrical specimens (ϕ10×h10) by machining — Annealing at 350℃, 30 min

2) Al-Mg-Si alloy (6063 aluminum alloy)

Elements	Si	Mn	Ti	Fe	Zn	Cr	Cu	Mg	Al
Mass %	0.46	0.02	0.01	0.2	0.02	0.01	0.03	0.54	Bal.

Hot extruded rod — Cylindrical specimens (ϕ10×h10) by machining

3) SUS 304 stainless steel

Elements	C	Si	Mn	P	S	Cr	Ni	Fe
Mass %	0.08	0.5	1.82	0.033	0.011	18.95	8.39	Bal.

Annealed rod — Cylindrical specimens (ϕ10×h10) by machining

pressive testings were proceeded. Deformation temperature (initial value) is measured by using the thermo-couple (alumel-cromel), attached to the test piece by a fine metal wire, and digital thermo-meter. Colloidal graphite (Oil-Dag) was used as lubricant. Figs. (5)–(8) show the flow curves measured by experiments performed at some constant strain-rates and at some constant temperatures. Those flow curves were referred to determine the values of material constants involved in the work-hardening rate equations.

4.2 σ_b–ε curve and γ_s–$\dot{\varepsilon}$ relation

Base temperature, T_o, is set to 301 K (28℃) and base strain-rate, $\dot{\varepsilon}_b$, to 1.0 s^{-1} (Aluminum and 6063 alloy) or 1.23 s^{-1} (SUS304 stainless steel), so that the prediction method can be applied to deformation at above 301 K. The values of material constant, γ_s, were determined at some strain-rates with referring the flow curves measured at 301 K (28℃). Fig. 9 shows the base flow curves, σ_b–ε curves. Flow curves at larger strain region than 0.7 are the results of extrapolation by using the equation, $\sigma=C_2\varepsilon^n$. Where, parameters, C_2 and n are determined with the flow stress and strain relations in strain, 0.4–0.7. Equations representing the base flow curve were written in the figure. Those equations were included in the computer prediction program of flow curves. Fig. 10 shows the material constants, γ_s, (represented by $\gamma_s/\dot{\varepsilon}$) and strain-rate $\dot{\varepsilon}$ relations.

4.3 γ_o and q

The values of material constants, γ_o and q, were determined with referring the flow curves measured at some strain-rates and some temperatures above room temperature. The results re-

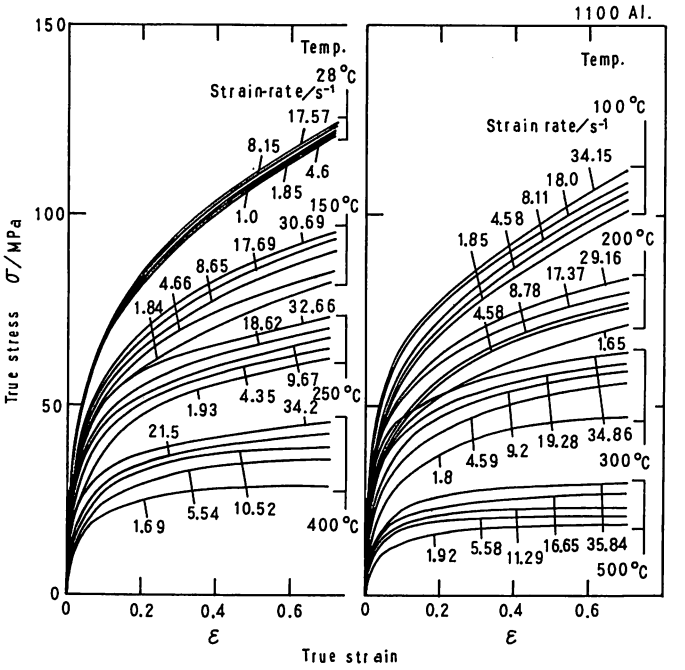

Fig. 5 Flow curves measured by experiments performed at some constant strain-rates and at some constant temperatures. (1100-0 Aluminum)

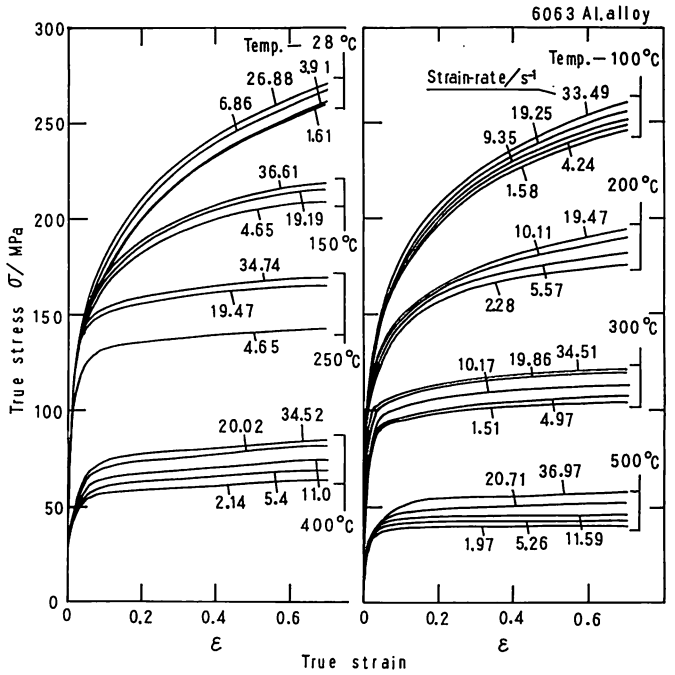

Fig. 6 Flow curves measured by experiments performed at some constant strain-rates and at some constant temperatures. (6063 Aluminum Alloy)

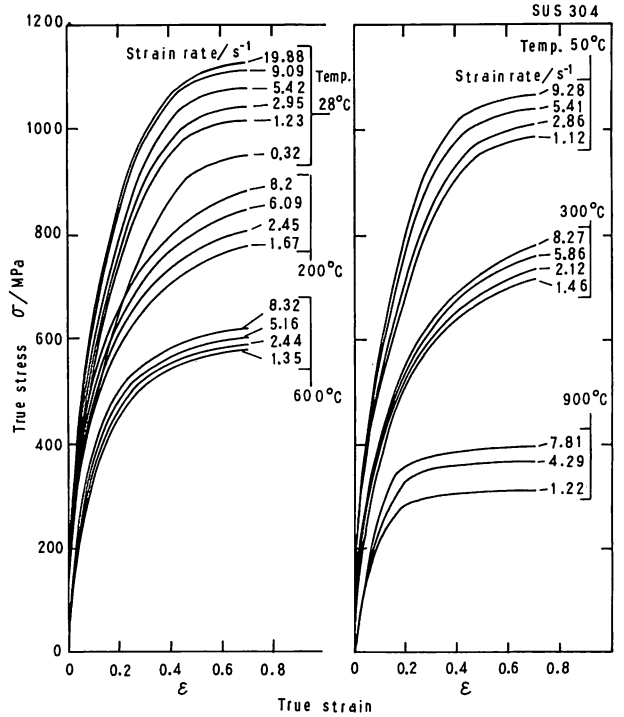

Fig. 7 Flow curves measured by experiments performed at some constant strain-rates and at some constant temperatures. (SUS304 Stainless Steel)

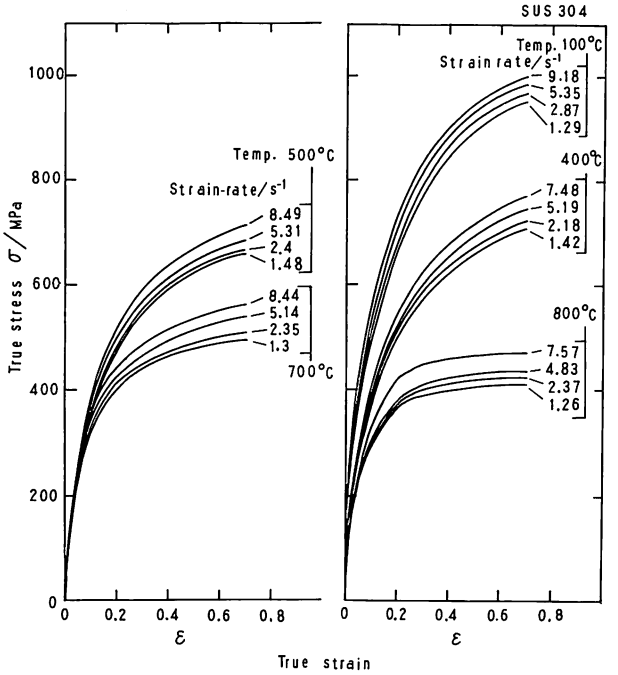

Fig. 8 Flow curves measured by experiments performed at some constant strain-rates and at some constant temperatures. (SUS304 Stainless Steel)

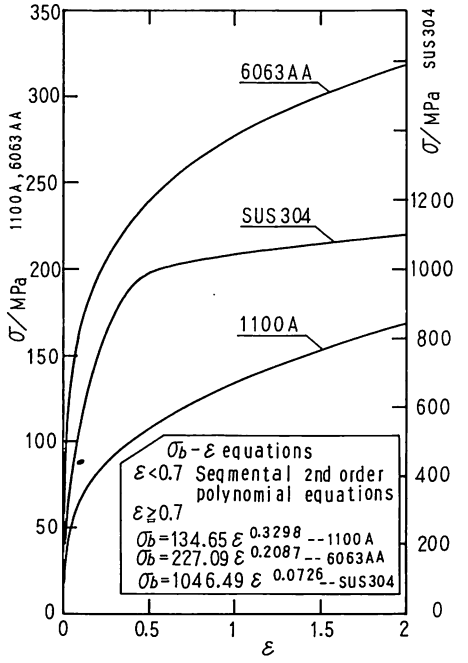

Fig. 9 σ_b–ε curves measured by experiments and σ_b–ε equations.
Base temperature, T_0=301K (28℃)
Base strain-rate: $\dot{\varepsilon}_b$=1.0s^{-1} (1100A, 6063AA)
$\dot{\varepsilon}_b$=1.23s^{-1} (SUS304)

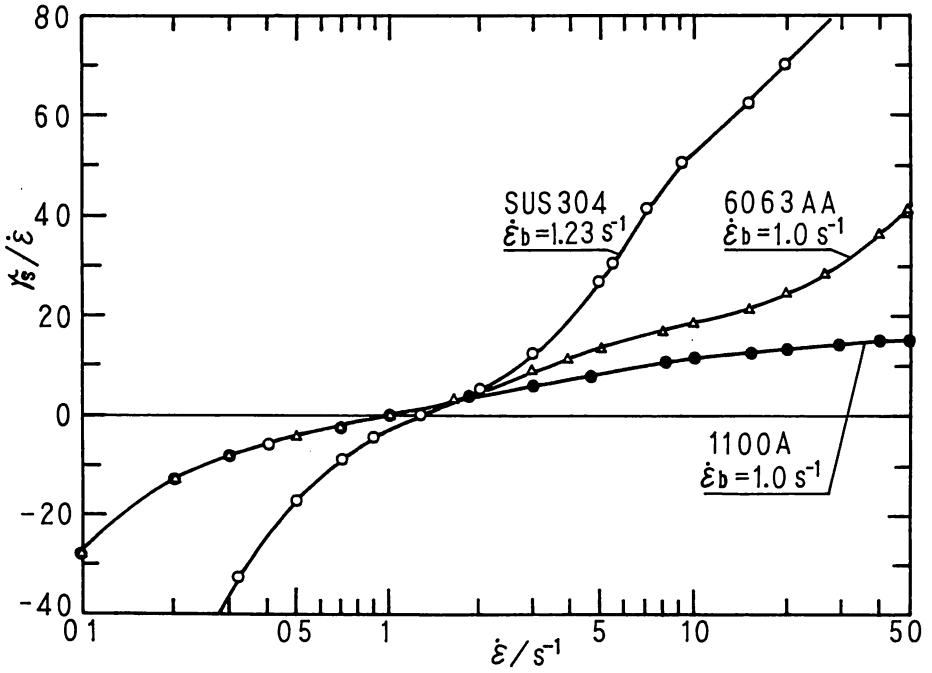

Fig. 10 $(\gamma_s/\dot{\varepsilon})-\dot{\varepsilon}$ **relations at base temperature,** T_o=301K (28℃).
Base strain-rate: $\dot{\varepsilon}_b$=1.0s^{-1} (1100A, 6063AA)
$\dot{\varepsilon}_b$=1.23s^{-1} (SUS304)

veal that relation between γ_o and both temperature and strain-rate can be written by eq.(7).

$$\gamma_o = A_1 \dot{\varepsilon}^{B_1} \quad \cdots\cdots\cdots\cdots (7)$$

Where, A_1 and B_1 are temperature dependents. Fig. 11 shows the values of A_1 and B_1 with regard to deformation temperature, t_e℃.

Fig. 12 shows material constant, q, with regard to the reciprocal of temperature, 1/T. Relation between q and 1/T can be represented by eq.(8).

$$q = C_1 \exp(D_1/T) \quad \cdots\cdots\cdots\cdots (8)$$

The values of the constants, C_1 and D_1, are written in the figure.

4.4 Computer program of flow curve prediction

The following results of analysis, a)-d), were included in the computer program of flow curve prediction shown in Fig. 1.

a) $\sigma_b-\varepsilon$ curve, which gives $(d\sigma_o/d\varepsilon)_{\varepsilon, \dot{\varepsilon}_b, T_o}$.
The curve was expressed by the segmental 2nd. order polynomial equations and power law equation in the program. (Ref. Fig. 9)

b) $(\gamma_s/\dot{\varepsilon})-\dot{\varepsilon}$ relation
The relation was expressed by the segmental 2nd. order polynomial equations in the program.

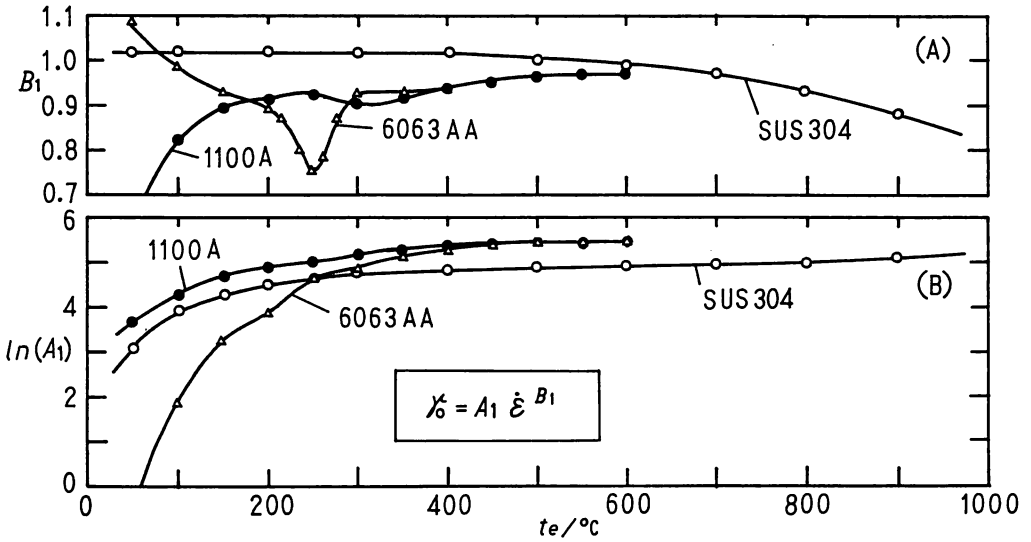

Fig. 11 The values of material constants, B_1 and $ln(A_1)$ in $\gamma_0 = A_1 \dot{\varepsilon}^{B_1}$ with regard to temperature, te.

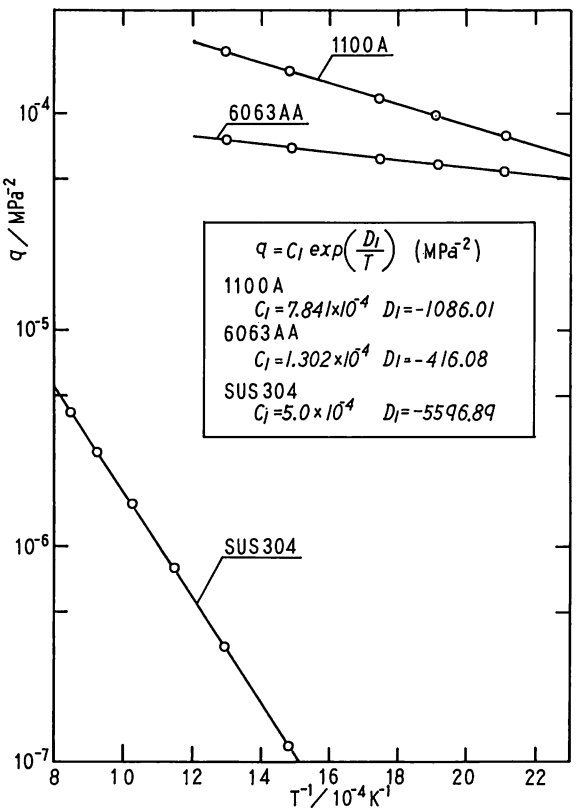

Fig. 12 $ln\ q-(1/T)$ linear relations.

c) A_1-t_e relation and B_1-t_e relation in $\gamma_0=A_1\dot{\varepsilon}^{B_1}$
The relations were expressed by the segmental 2nd. order polynomial equations in the program.

d) $q-(1/T)$ relation

$q = 7.841\times10^{-4}\exp(-1086.01/T)$, for Aluminum

$q = 1.302\times10^{-4}\exp(-416.08/T)$, for Al-Mg-Si alloy

and $q = 5.0\times10^{-4}\exp(-5596.89/T)$, for SUS304 stainless steel

4.5 Verification of the computer prediction program

Figs. (13)–(14) show the flow curves calculated by the computer program shown by Fig. 1 in which the equations representing the $\sigma_b-\varepsilon$ curve, $(\gamma_s/\dot{\varepsilon})-\dot{\varepsilon}$ relation, A_1-t_e relation and B_1-t_e relation in $\gamma_0=A_1\dot{\varepsilon}^{B_1}$ and $q-(1/T)$ relation are included. Solid lines represent the flow curves calculated by the computer program and the open circles plotted are the results of experiments. Flow curves calculated are verified to coincide with the results of experiments. Fig. 15 shows comparison of the flow curves which were calculated in deformation condition of isothermal or of adiabatic. Two initial deformation conditions were assumed; i.e., deformation conditions of t_e=200℃ and $\dot{\varepsilon}=30.7\,s^{-1}$ and those of t_e=400℃ and $\dot{\varepsilon}=34.52\,s^{-1}$. The open circles plotted are the results of experiments proceeded by using the cam-plasto meter. Sub-press may keep deformation temperature constant. Fig. 15 shows that the flow curves predicted in deformation condition of isothermal coincide with the experimental results plotted by the open circles. Effect of adiabatic temperature rise due to plastic working energy on flow stress is much remarkable at 200℃ than at 400℃.

Furthermore, flow curves were predicted by the computer program in deformation conditions with varying strain-rates and constant temperatures. Fig. 16 shows the results. Solid

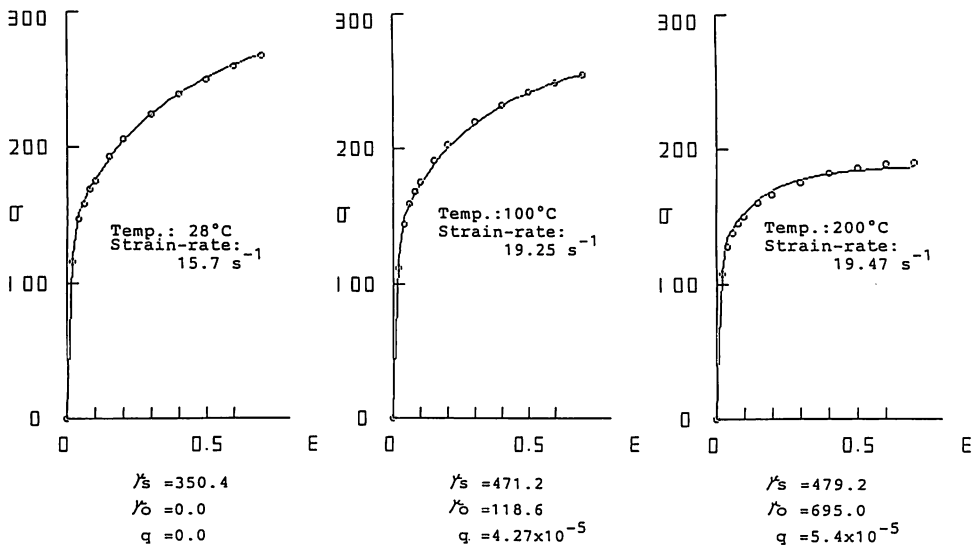

Fig. 13 Comparison of the predicted flow curves with experimental data.
—— : Calculated by using the computer prediction program
○ : Experimental data (σ MPa) (6063 Aluminum Alloy)

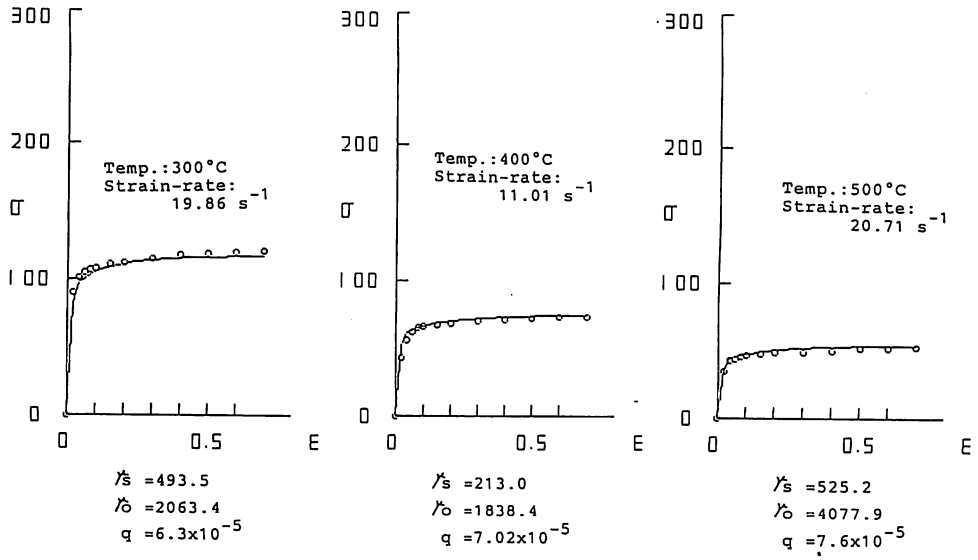

Fig. 14 Comparison of the predicted flow curves with experimental data.
—— : Calculated by using the computer prediction program
○ : Experimental data (σ MPa) (6063 Aluminum Alloy)

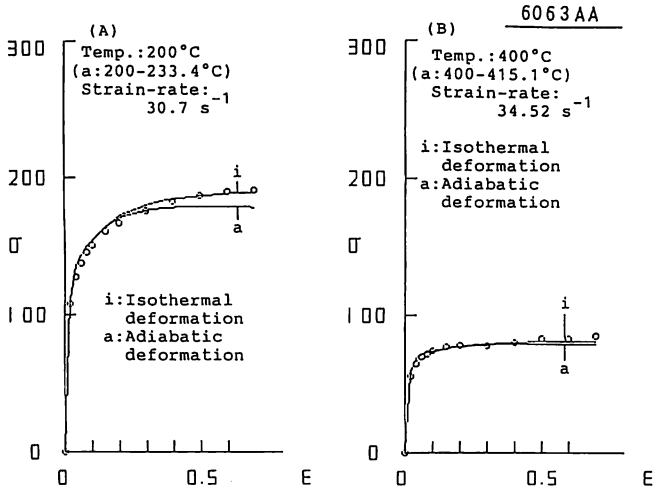

Fig. 15 Examples of the flow curve prediction in isothermal deformation and in adiabatic deformation. (6063 Aluminum Alloy)

lines in (B) are flow curves calculated at temperatures, 200℃ or 400 ℃ or 500 ℃ and strain-rate variations, $\dot{\varepsilon}_1$ or $\dot{\varepsilon}_2$ or $\dot{\varepsilon}_3$ or $\dot{\varepsilon}_4$ shown in (A). Open circles plotted in the same figure represent the flow stresses at some strains measured by the experiments performed at the same deformation conditions as those of calculation.

5. Conclusions

Numerical calculation method for predicting the flow curves by using the work-hardening

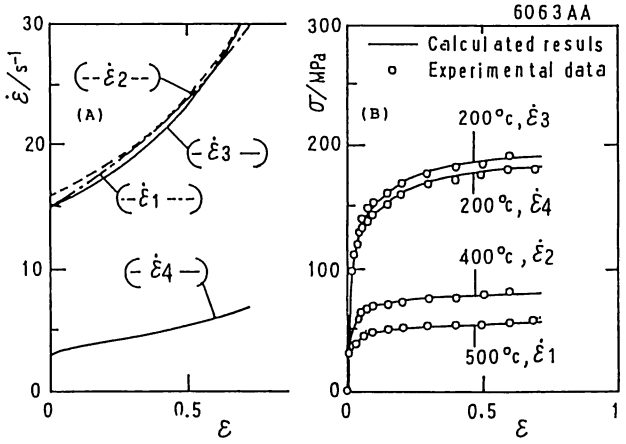

Fig. 16 Examples of the flow curve prediction.
[Deformation conditions are varying strain-rates in isothermal deformation.]
(A) : Strain-rate conditions, (B) : Flow curves
(6063 Aluminum Alloy)

rate equations was applied to flow stress prediction of Aluminum (1100-0 aluminum), Al-Mg-Si alloy (6063 aluminum alloy) and SUS304 stainless steel. Then, the work-hardening rate equations involving some material constants could be determined for the above materials and the computer program of flow curve prediction was constructed. Some flow curves measured by experiments and those predicted by the present program were compared and excellent agreement was confirmed. The prediction program of flow curves can be adopted to stress analysis of a forming process and to a numerical forming simulation.

Acknowledgements

Financial support of the Ministry of Education, Japan, for scientific research, Grant No. 04650633, is gratefully acknowledged.

References

(1) Dadras, P.: Trans. ASME, J. Eng. Mater. Technol., 107 (1985), p. 97.
(2) Yada, H. and Senuma, T.: J. JSTP, (塑性と加工), 27-300 (1986), p. 34.
(3) Marciniak, Z. and Konieczny, A.: J. Mech. Working Technol., 15 (1987), p. 15.
(4) Nakanishi, K. : Res. Report, the Faculty of Eng., Kagoshima University, 30 (1988), p. 13.
(5) Nakanishi, K.: J. JSTP, (塑性と加工), 30-337 (1989), p. 262.
(6) Brown, S. B., Kim, K. H., and Anand, L.: Int. J. Plasticity, Vol. 5 (1989), p. 95.
(7) Yoshino, M. and Shirakashi, T.: J. JSTP, (塑性と加工), 31-359 (1990), p. 1433, p. 1439.
(8) Laasraoui, A. and Jonas, J. J.: Met. Trans., 22A (1991), p. 1545.
(9) Miyagawa, H., Nakajima, E. and Yoshinaga, H.: J. JIM, (日本金属学会誌), 56-5 (1992), p. 531.